Numerical Simulation of Fluid Flow and Time-Lapse Seismics Applied to CO_2 Sequestration at the Sleipner-field

J. E. Santos[1]

[1] Department of Mathematics, Purdue University,

IGPUBA, Fac. Ing., UBA and Univ. Nac. de La Plata, ARGENTINA

Work with G. B. Savioli (IGPUBA), J. M. Carcione and D. Gei ((OGS), Trieste, ITALY).

GEOTECHNICAL WORKSHOP ON ENERGY GEOTECHNICS, PURDUE GEOTECHNICAL SOCIETY, April 26, 2014

troduction. I

- Storage of CO_2 in geological formations is a procedure employed to reduce the amount of greenhouse gases in the atmosphere to slow down global warming.
- Geologic sequestration involves injecting CO_2 into a target geologic formation at depths typically >1000 m where pressure and temperature are above the critical point for CO_2 (31.6C, 7.38 MPa).
- First industrial scale CO_2 injection project: Sleipner gas field (North Sea).

troduction. II

- CO_2 is separated from natural gas produced and is currently being injected into the Utsira Sand, a saline aquifer at the Sleipner field, some 26000 km^2 in area.
- Injection started in 1996 at a rate of about one million tonnes per year.
- Time-lapse seismic surveys aim to monitor the migration and dispersal of the CO_2 plume after injection.
- Very little is known about the effectiveness of CO_2 sequestration over very long periods of time.

troduction. III

- The analysis of CO_2 underground storage safety in the long term is a current area of research.
- We present a methodology integrating numerical simulation of CO_2-brine flow and seismic wave propagation to model and monitor CO_2 injection.
- The model of the formation is based on the porosity and clay content distribution considering the variation of properties with fluid pressure and saturation.
- The model considers the geometrical features of the formations, including the presence of shale seals and fractures and fractal variations of the petrophysical properties.

resentation Outline

- Present the two-phase fluid flow equations used to simulate CO_2 injection.
- Describe a viscoelastic model for wave propagation
- Present a petrophysical model of a shaly sandstone based on fractal porosity and clay content, considering the variation of properties with pressure and saturation.
- Show numerical simulations of CO_2 injection and time-lapse seismics to monitor the migration and dispersal of CO_2 after injection in the Utsira formation at the Sleipner field in the North Sea.

he Black-Oil formulation

- The simultaneous flow of brine and CO_2 is described by the well-known **Black-Oil formulation** applied to two-phase, two component fluid flow.
- In the **Black-Oil** model employed, brine is NOT present, OIL is identified with brine and CO_2 is identified with GAS.
- Also, CO_2 may dissolve in brine (OIL) but brine (OIL) is not allowed to vaporize into the CO_2 phase.
- This formulation uses, as a simplified thermodynamic model, the quantities R_s, B_b and B_{CO2} as PVT data:

e Black-Oil formulation of two-phase flow in porous media. I

- $R_s = \frac{V_{dCO2}^{SC}}{V_b^{SC}}$: CO_2 solubility in brine
- $B_{CO2} = \frac{V_{CO2}^{res}}{V_{CO2}^{SC}}$: CO_2 formation volume factor
- $B_b = \frac{(V_{dCO2}^{res} + V_b^{res})}{V_b^{SC}}$: brine formation volume factor

o estimate the above PVT data we used an algorithm developed by assanzadeh (2008).

he Black-Oil equations for two-phase flow in porous media are obtained ombining conservation of mass of each component with two-phase arcy's law.

e Black-Oil formulation of two-phase flow in porous media. II

$$\nabla \cdot \left[\frac{\underline{\kappa} k_{rCO2}}{B_{CO2}\eta_{CO2}} (\nabla p_{CO2} - \rho_{CO2} g \nabla D) + \frac{\underline{\kappa} R_s k_{rb}}{B_b \eta_b} (\nabla p_b - \rho_b g \nabla D) \right]$$

$$+ q_{CO2} = \frac{\partial \left[\phi \left(\frac{S_{CO2}}{B_{CO2}} + \frac{R_s S_b}{B_b} \right) \right]}{\partial t}$$

$$\nabla \cdot \left[\frac{\underline{\kappa} k_{rb}}{B_b \eta_b} (\nabla p_b - \rho_b g \nabla D \right] + q_b = \frac{\partial \left[\phi \frac{S_b}{B_b} \right]}{\partial t}$$

wo algebraic equations complete the system:

$$S_b + S_{CO2} = 1, \qquad p_{CO2} - p_b = P_C(S_b)$$

merical solution of the Black-Oil formulation of two-phase flow in poro

he unknowns for the Black-Oil fluid-flow model are the fluid pressures
$_{CO2}, p_b$ and the saturations S_{CO2}, S_b for the CO_2 and brine phases.

hey were computed using the public domain software BOAST, which
olves the differential equations applying IMPES, a finite difference
chnique.

smic modeling. Mesoscopic attenuation effects. I

- An important mechanisms of P-wave attenuation and dispersion at seismic frequencies is known as mesoscopic loss, due to heterogeneities larger than the pore size but much smaller than the predominant wavelengths (mesoscopic-scale heterogeneities).
- These effects are due to the equilibration of wave-induced fluid pressure gradients via a slow-wave diffusion process (Type II Biot waves).
- White et al. (1975) were the first to introduce the mesoscopic-loss mechanism in the framework of Biot's theory, which is illustrated in the next figures.

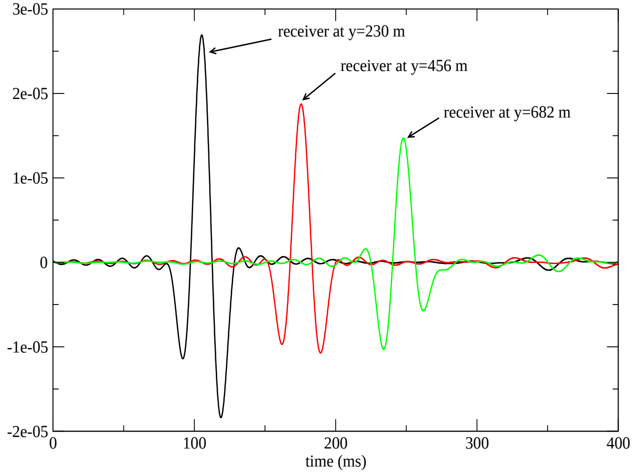
receiver at y=230 m
receiver at y=456 m
receiver at y=682 m
3e-05
2e-05
1e-05
0
-1e-05
-2e-05
0
100
200
300
400
time (ms)

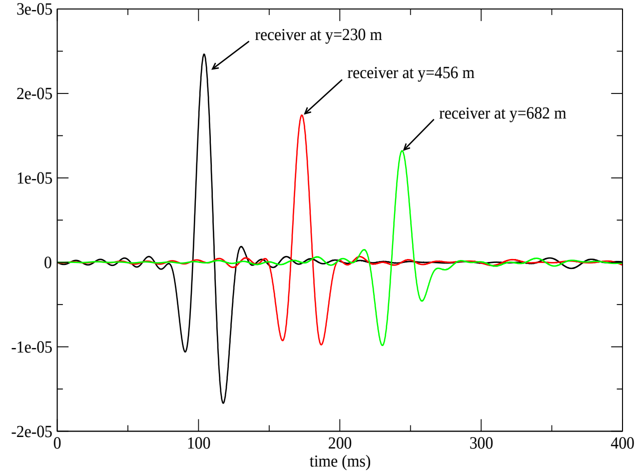
receiver at y=230 m
receiver at y=456 m
receiver at y=682 m
3e-05
2e-05
1e-05
0
-1e-05
-2e-05
0
100
200
300
400
time (ms)

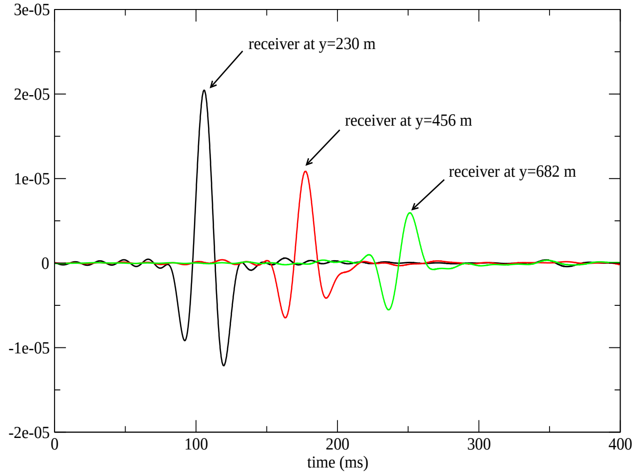
receiver at y=230 m
receiver at y=456 m
receiver at y=682 m
3e-05
2e-05
1e-05
0
-1e-05
-2e-05
0
100
200
300
400
time (ms)

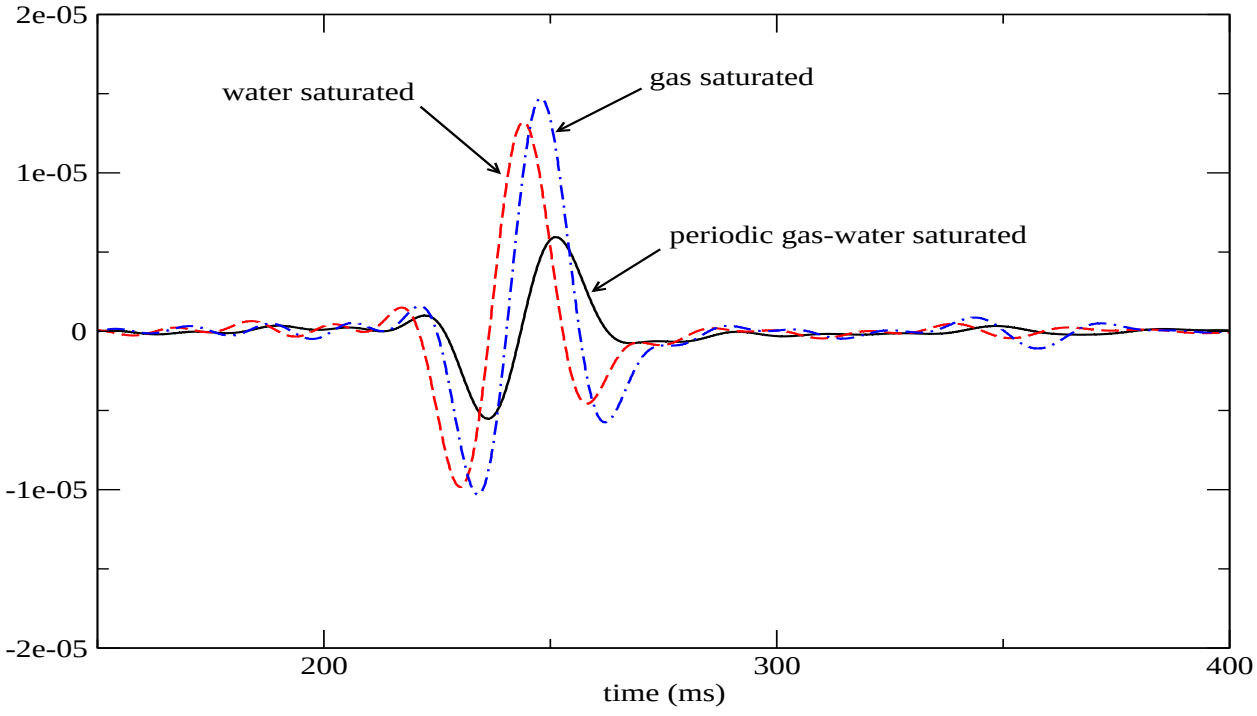

The delay in the arrival time in the periodic case is due to the velocity dispersion caused by the esoscopic scale heterogeneities. Attenuation and dispersion in the periodic gas-water case is in perfect agreement with that predicted by White's theory.

smic modeling. Mesoscopic attenuation effects. II

- Due to the extremely fine meshes needed to properly represent these type of media, numerical simulations at the macroscale is very expensive or even not feasible.
- Our approach: employ an upscaling procedure to include the mesoscale effects in the macroscale.
- At the bottom and top of the Utsira formation and in the mudstone layers inside the Utsira formation the complex bulk and shear moduli as function of frequency were determined using a Zener model.

- Within the Utsira formation and outside the mudstone layers, we determine complex and frequency dependent P-wave modulus

$$E(\omega) = \lambda(\omega) + 2\mu(\omega)$$

  at the mesoscale using White's theory for patchy saturation.
- $\lambda(\omega), \mu(\omega)$: Lamé coefficients
- ω : angular frequency

- Shear wave attenuation is taken into account using another relaxation mechanism related to the P-wave White mechanism to make the shear modulus

$$\mu(\omega)$$

complex and frequency dependent.

- These complex moduli define an equivalent viscoelastic model at the macroscale that take into account dispersion and attenuation effects occuring at the mesoscale.

$= u(\omega) = (u_x(\omega), u_z(\omega))$: **Time-Fourier transform of the displacement ector**

tress-strain relations in the space-frequency domain:

$$\sigma_{jk}(u) = \lambda(\omega)\nabla \cdot u\delta_{jk} + 2\mu(\omega)\varepsilon_{jk}(u),$$

$_{jk}(u)$: **stress tensor** $\varepsilon_{jk}(u)$: **strain tensor**

$_k$: **Kroenecker delta**

smic modeling. Phase velocities and attenuation coefficient.

or isotropic viscoelastic solids, the frequency dependent phase elocities $v_t(\omega)$ and quality factors $Q_t(\omega)$, $t = p, s$ are defined by the lations

$$v_t(\omega) = \left[\mathrm{Re}\left(\frac{1}{vc_t(\omega)}\right)\right]^{-1}, \; Q_t(\omega) = \frac{\mathbf{Re}(vc_t(\omega)^2)}{\mathbf{Im}(vc_t(\omega)^2)}, \;\; t = p, s$$

$c_p(\omega), vc_s$: complex and frequency dependent compressional and shear elocities defined as

$$vc_p(\omega) = \sqrt{\frac{E(\omega)}{\rho}}, \quad vc_s(\omega) = \sqrt{\frac{\mu(\omega)}{\rho}}$$

bulk density.

quation of motion in a 2D isotropic viscoelastic domain Ω with boundary Ω:

$$\omega^2 \rho u + \nabla \cdot \sigma(u) = f(x,\omega), \quad \Omega$$
$$-\sigma(u)\nu = i\omega \mathcal{D} u, \quad \partial\Omega,$$

(x,ω) external source

$$\mathcal{D} = \rho \begin{bmatrix} \nu_1 & \nu_2 \\ -\nu_2 & \nu_1 \end{bmatrix} \begin{bmatrix} v_p(\omega) & 0 \\ 0 & v_s(\omega) \end{bmatrix} \begin{bmatrix} \nu_1 & -\nu_2 \\ \nu_2 & \nu_1 \end{bmatrix},$$

$= (\nu_1, \nu_2)$: the unit outward normal on Γ

merical Solution - Finite Element Method.

- The FE was computed at a selected number of frequencies in the range of interest using an iterative finite element domain decomposition procedure.
- The time domain solution was obtained using a discrete inverse Fourier transform.
- To approximate each component of the solid displacement vector we employed a nonconforming finite element space which generates less numerical dispersion than the standard bilinear elements.
- The error measured in the energy norm is of order $h^{1/2}$, where h is the size of the computational mesh.

etrophysical model for the Utsira formation. I

he pressure dependence of the petrophysical properties:

$$\frac{(1-\phi_c)}{K_s}(p(t)-p_H) = \phi_0 - \phi(t) + \phi_c \ln\frac{\phi(t)}{\phi_0}, \qquad (1)$$

$(t) = S_b p_b(t) + S_g p_g(t)$ **: pore pressure,**

$_c$**: critical porosity**

$_0$ **the initial porosity at hydrostatic pore pressure** p_H

$_s$**: the bulk modulus of the solid grains**

etrophysical model for the Utsira formation. II.

elationship among horizontal permeability κ_x porosity ϕ and clay ontent C is

$$\frac{1}{\kappa_x} = \frac{45(1-\phi)^2}{\phi^3}\left(\frac{(1-C)^2}{R_q^2} + \frac{C^2}{R_c^2}\right)$$

$_q$, R_c: average radii of sand and clay particles As permeability is nisotropic, we assume the following relationship between horizontal and ertical permeability κ_z

$$\frac{\kappa_x}{\kappa_z} = \frac{1-(1-0.3a)\sin\pi S_b}{a(1-0.5\sin\pi S_b)}$$

permeability-anisotropy parameter

etrophysical model for the Utsira formation. III.

he bulk modulus of the dry matrix was determined using a Krief model
$A = 4.5$**):**

$$K_m = K_s(1-\phi)^{A/(1-\phi)}.$$

K_s**: bulk modulus of the solid grains.**

ssuming a Poisson medium the shear modulus of the solid grains is
$\mu_s = 3K_s/5$ **and the following relation gives the shear modulus of the dry atrix**

$$\mu_m = \mu_s(1-\phi)^{A/(1-\phi)}.$$

odel for the Utsira formation.

- The model of the Utsira formation has 1.2 km in the x-direction, 10 km in the y-direction and 0.4 km in the z-direction (top at 0.77 km and bottom at 1.17 km b.s.l.).
- The pressure-temperature conditions are $T = 31.7z + 3.4$, where T is the temperature (in $^{\circ}$C) and z is the depth (in km b.s.l.); $p_H = \rho_b g z$ is the hydrostatic pressure, with ρ_b = 1040 kg/m^3 the density of brine and g the gravity constant.
- Within the formation, there are several mudstone layers which act as barriers to the vertical motion of the CO_2.

nodel for the Utsira formation. Initial porosity before CO_2 injection.

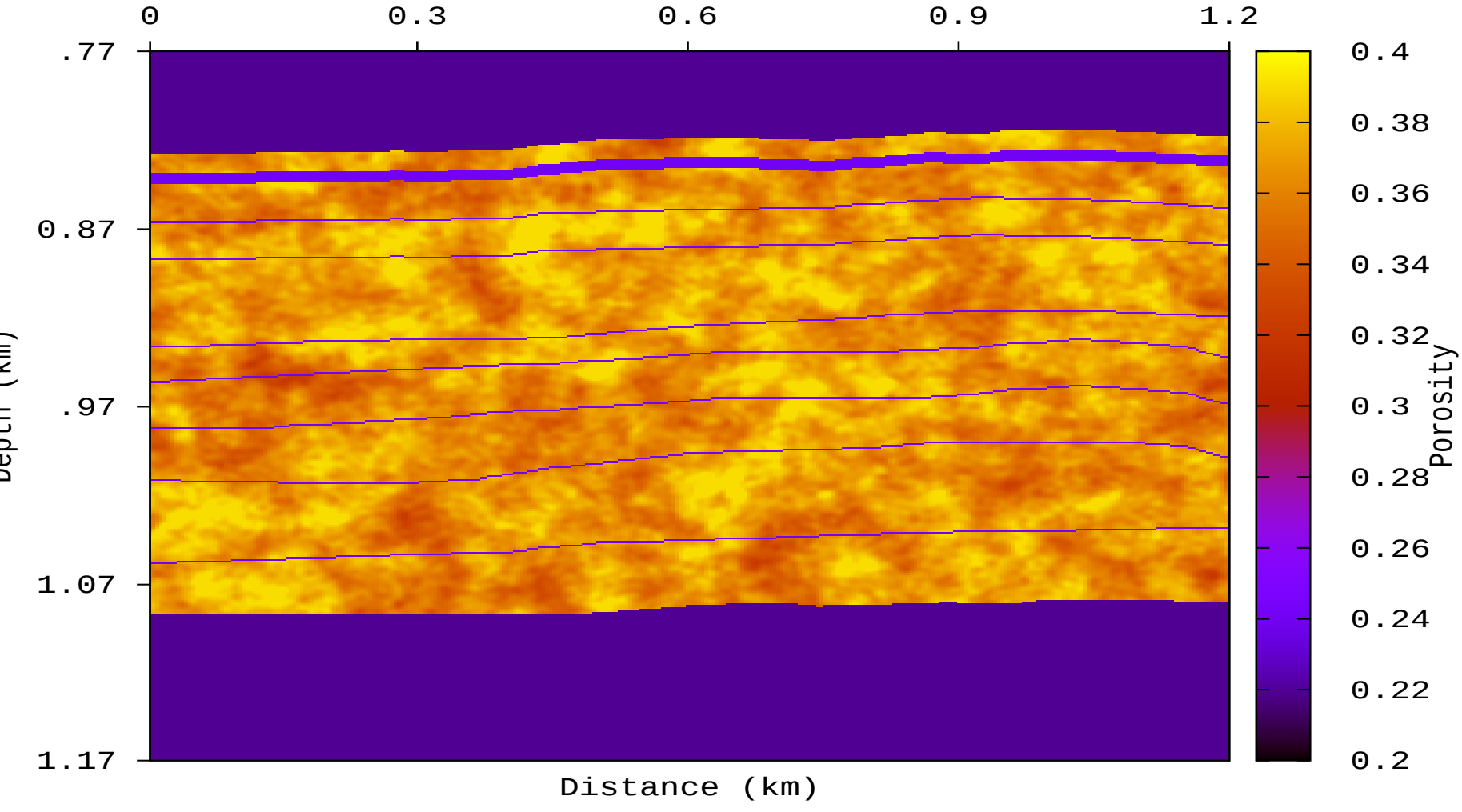

meability map (mD units) of the formation.

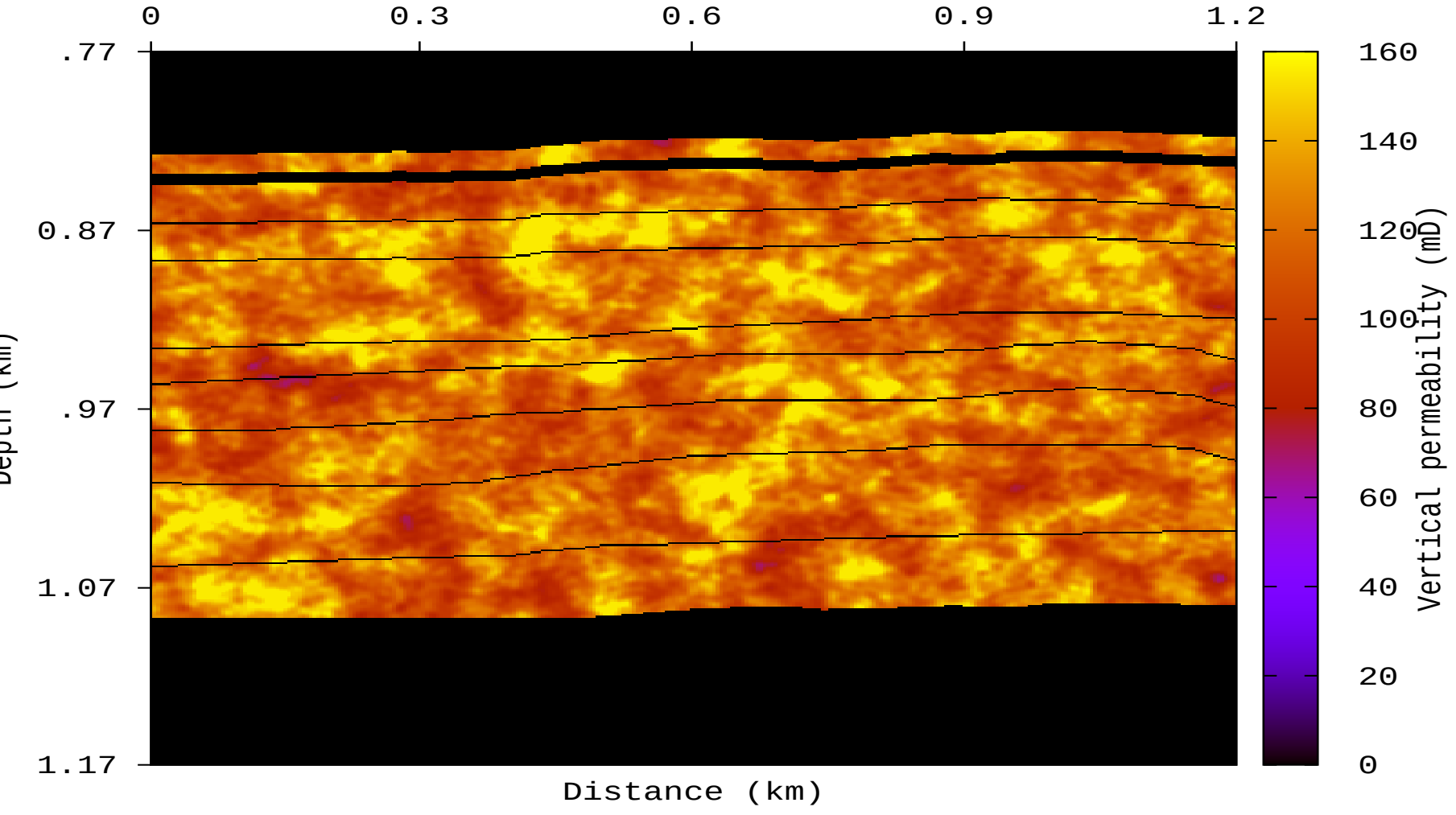

CO_2 Injection model. I

- At the Utsira formation CO_2 is injected at a constant flow rate of one millon tons per year.
- The injection point is located at the bottom of the Utsira formation: $x = 0.6$ km, $z = 1.06$ km.
- The viscosity, density and bulk modulus of CO_2 needed for the flow simulator were obtained from the Peng-Robinson equations as a function of temperature and pore pressure.

ection Modeling. II

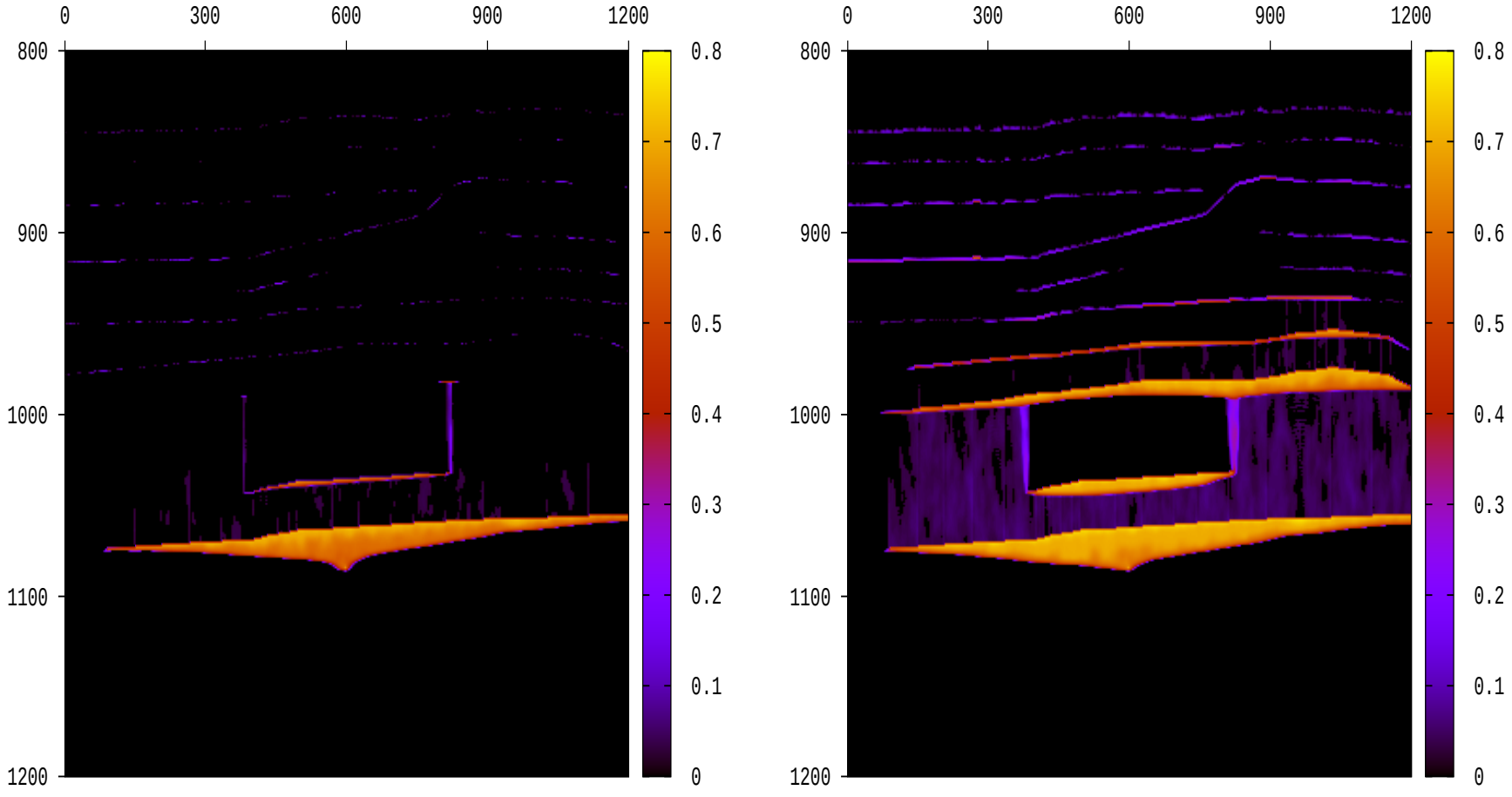

CO_2 saturation distribution after 2 years (left) and 6 years(right) of CO_2 injection

ismic Model.

- The equivalent viscoelastic model, determined using White's model for patchy saturation, assumes an effective single-phase fluid.
- Effective fluid density, viscosity and bulk modulus were obtained using the properties of the CO_2 and brine weighted by the corresponding saturations computed by the BOAST flow simulator.
- The next Figure displays maps of of P-wave phase velocity $v_p(\omega)$ and attenuation coefficient $Q_p(\omega)$ at 50 Hz after 2 years of CO_2 injection.

ve phase velocity $v_p(\omega)$(m/s) (left) and attenuation coefficient $Q_p(\omega)$ (right) at 50 Hz.

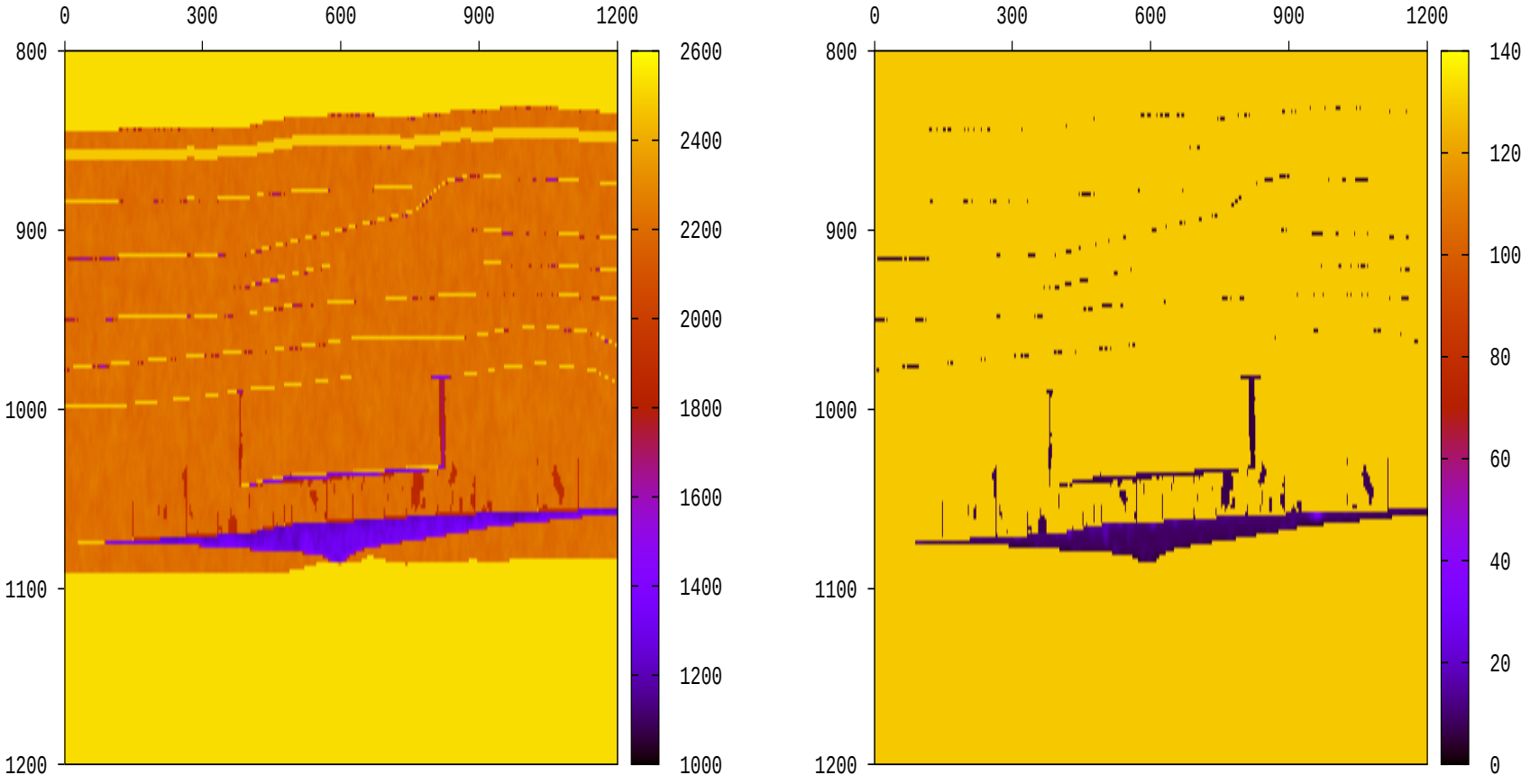

bserve a decrease in P- wave velocity in zones of CO_2 accumulation (left) and a corresponding decrease in attenuation coeefficient Q_p (right) .

ve phase velocity $v_s(\omega)$(m/s) (left) and attenuation coefficient $Q_s(\omega)$ (right) at 50 Hz.

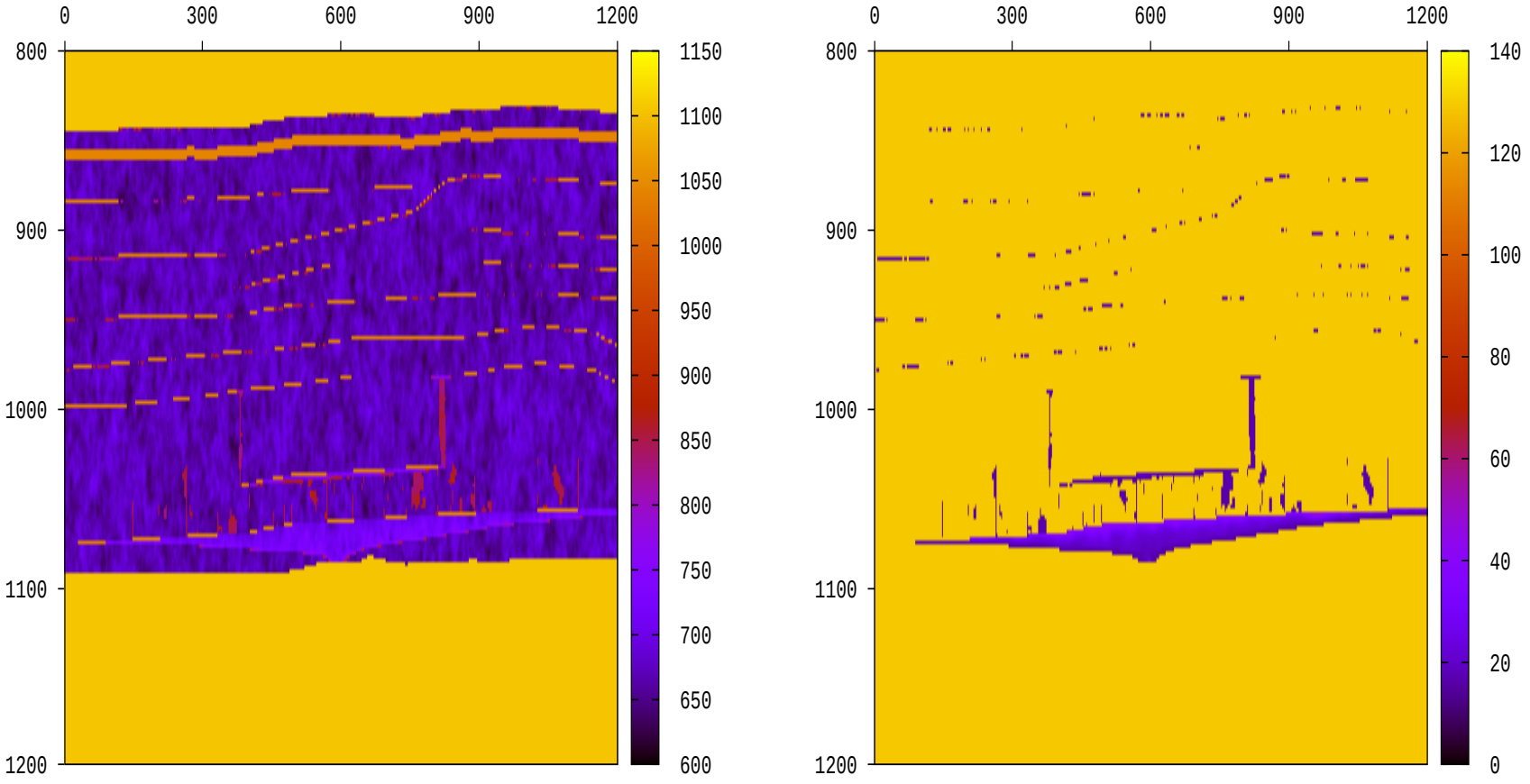

bserve a decrease in S- wave velocity in zones of CO_2 accumulation (left) and a corresponding decrease in attenuation coeefficient Q_s (right) .

ismic Monitoring.

- To analyze the capability of seismic monitoring to identify zones of CO_2 accumulation, the model was excited with compressional point and line sources located at the top of the model (800 m depth) with central frequency 50 Hz.
- The viscoelastic wave equation was solved for 200 frequencies. The time domain solution was obtained using an inverse Fourier transform.
- The next Figures display snapshots at several steps of the simulations. Other Figures show time histories before and after 2 and 6 years of CO_2 injection.

shots of z-component of particle velocity at 100 ms (left) and 150 ms (right). Point Source.

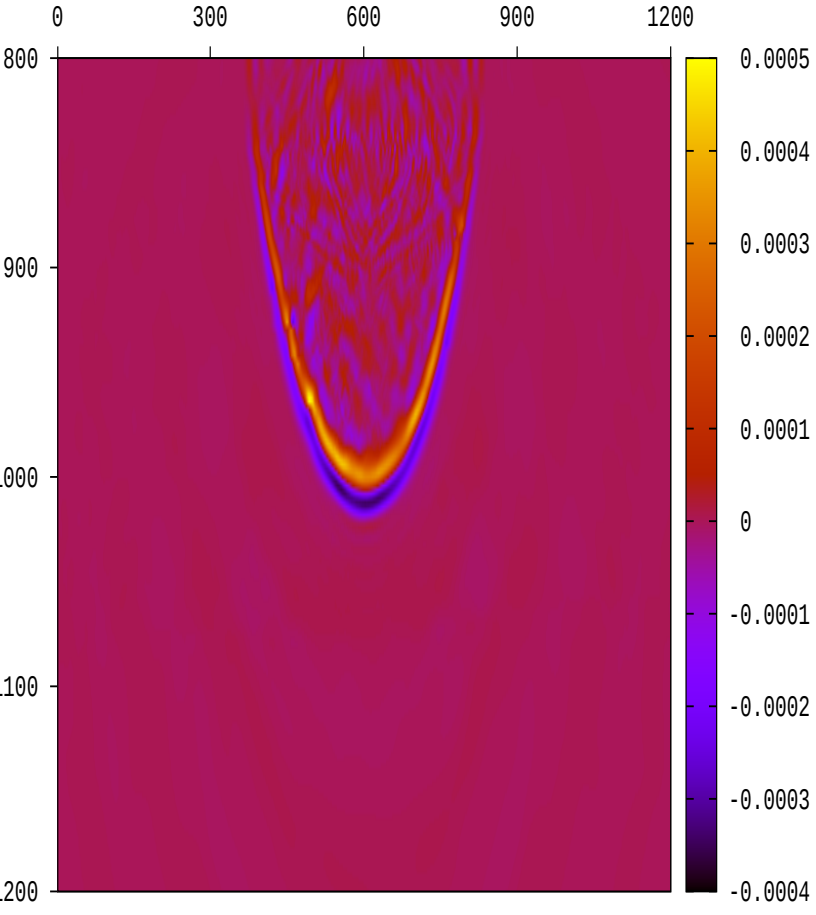

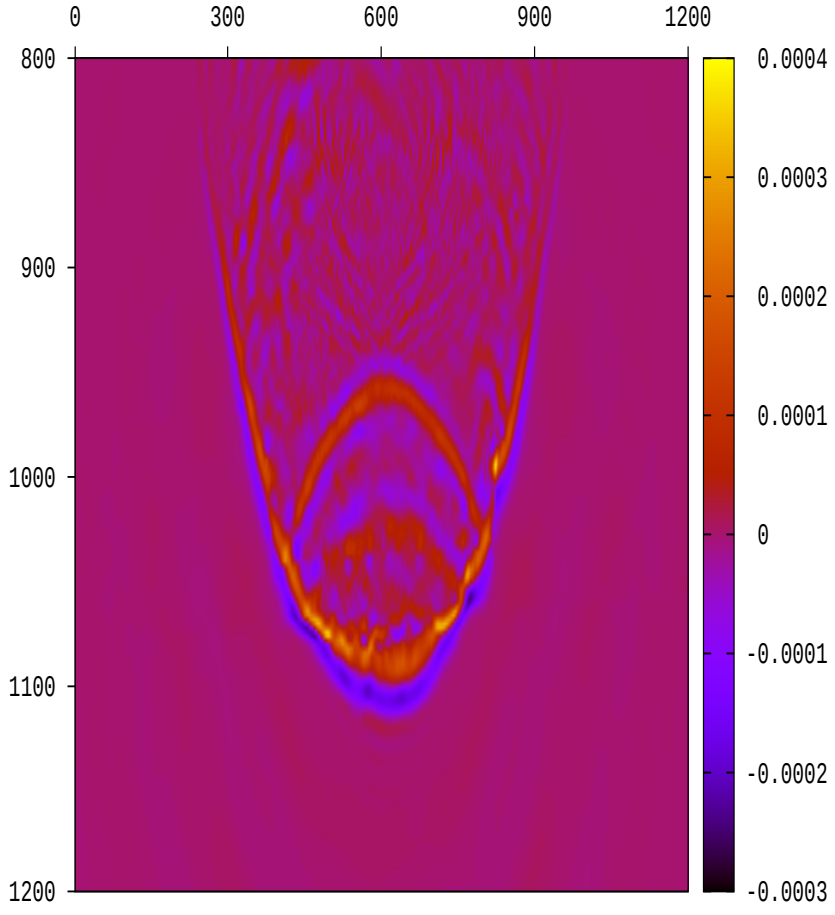

shots of z-component of particle velocity at 180 ms (left) and 200 ms (right). Point Source.

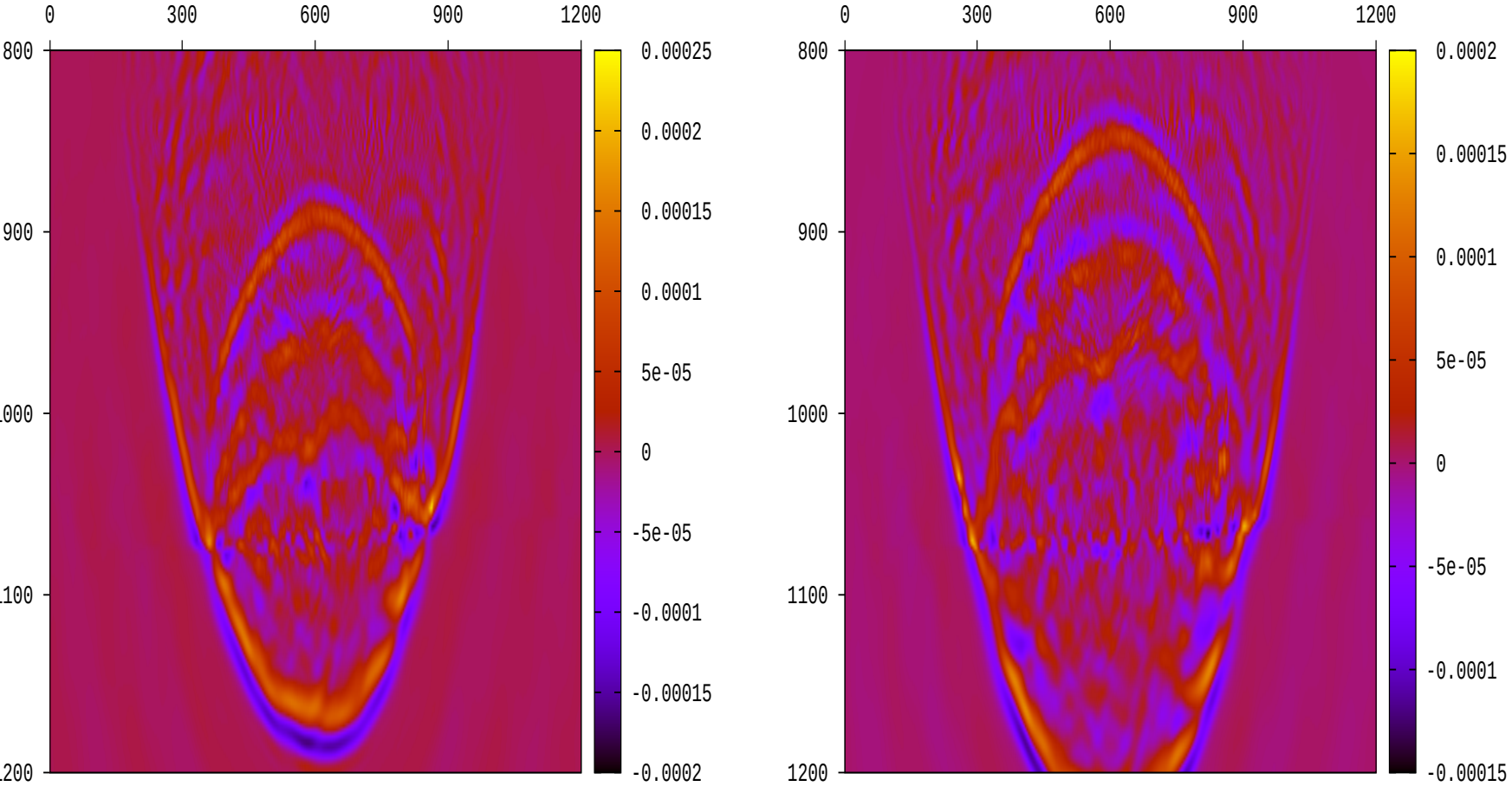

shots of z-component of particle velocity at 220 ms (left) and 280 ms (right). Point Source.

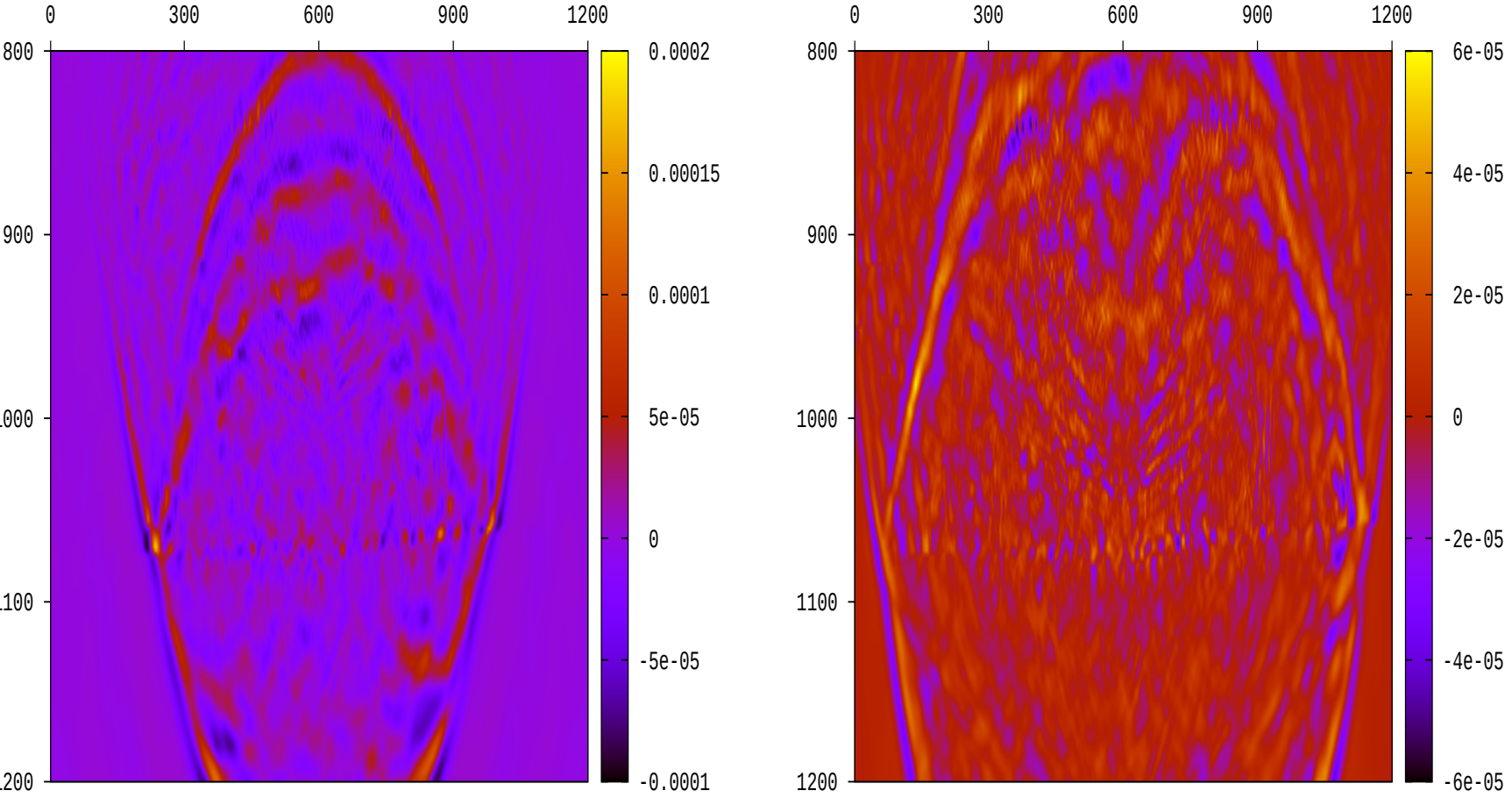

histories of the z-component of the particle velocity measured at the top of the model before and after 2 yea

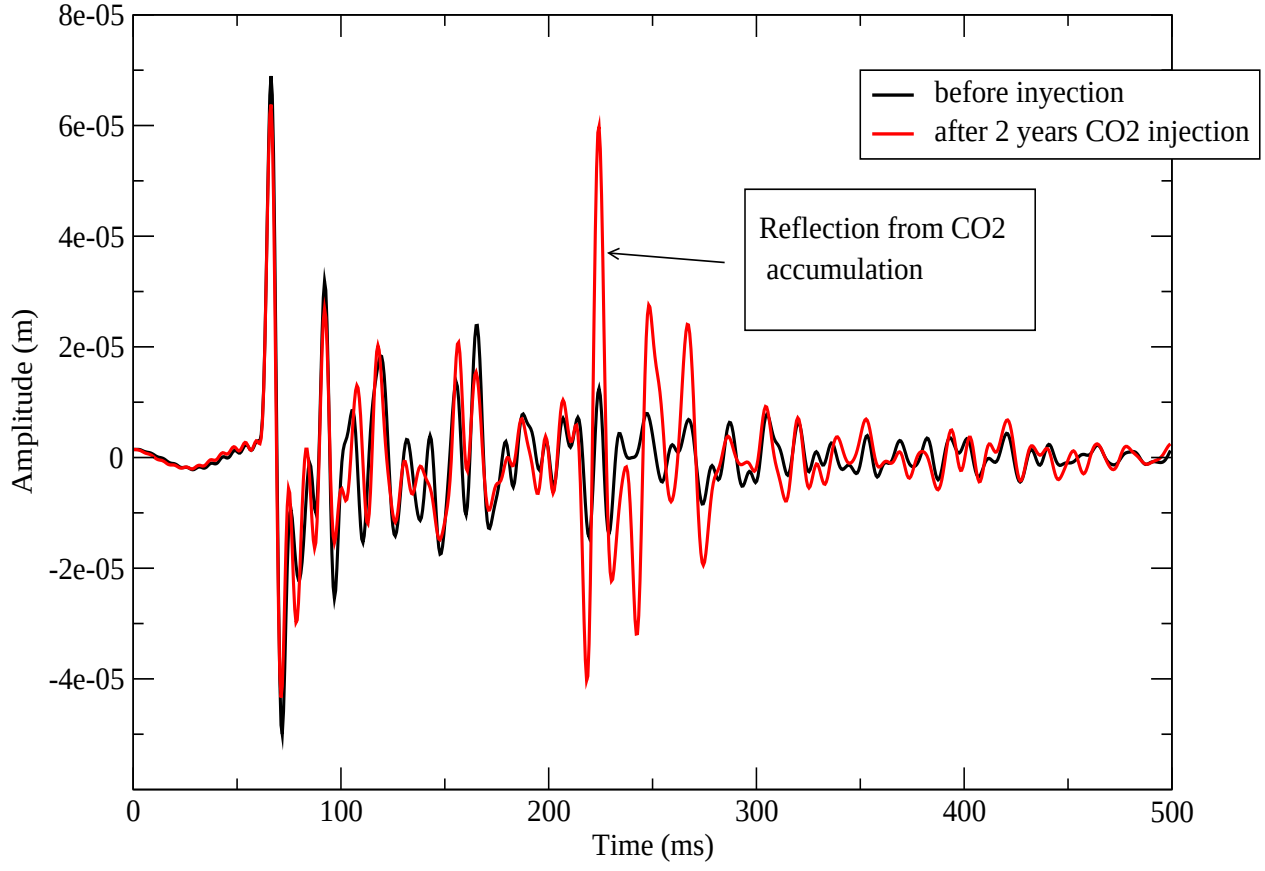

histories before and after 2 years of CO_2 injection. Point Source. Both figures are shown with the SAME S

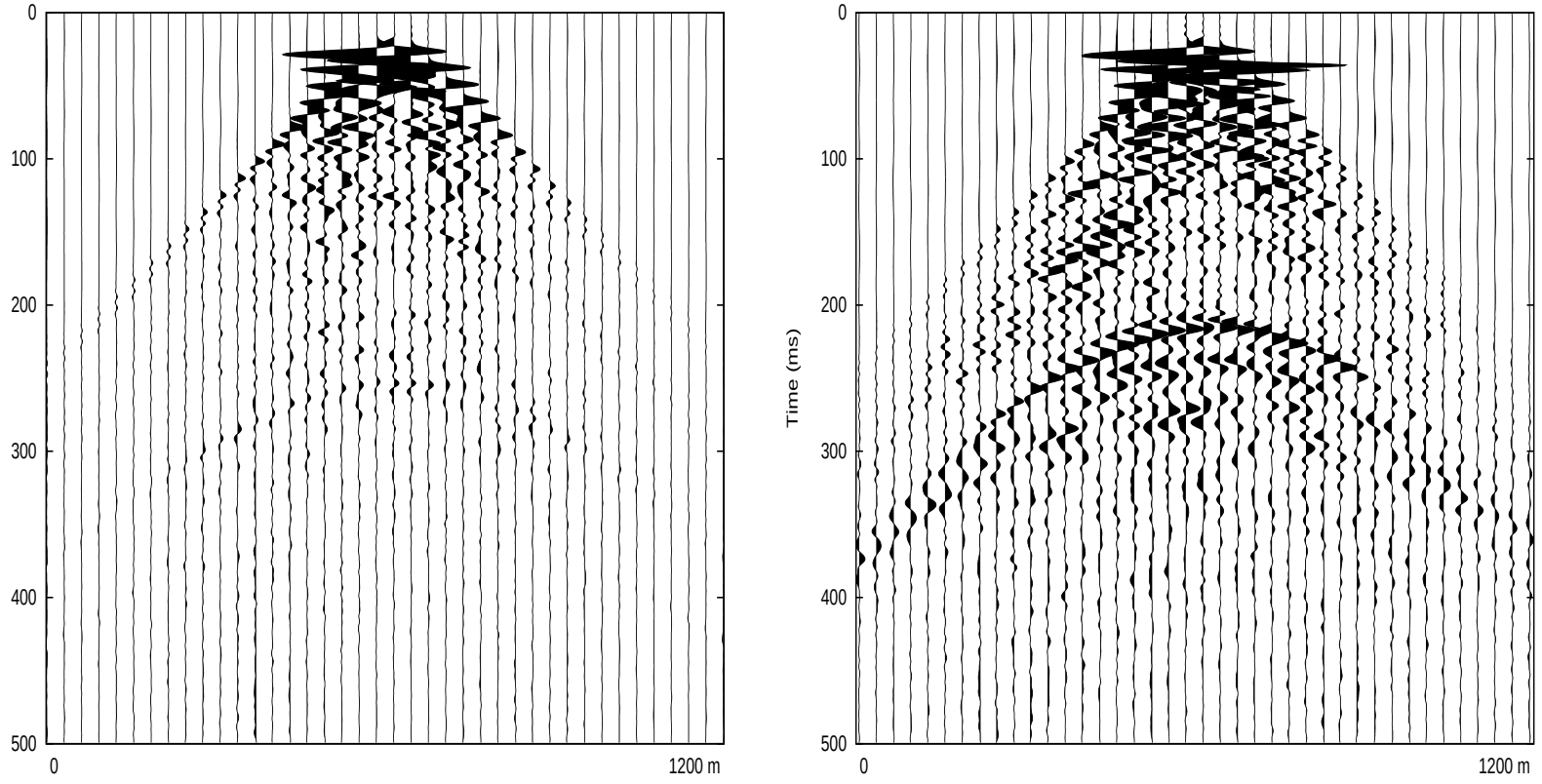

ces of the z-component of the velocity before (left) and after 2 years (right) CO_2 injection. The first strong

d second weak arrivals seen on the left Figure come from the base and top of the Utsira. The strong later

ivals seen on the right Figure are due to P-waves reflected at the CO_2 accumulations and the base of the

sira.

histories before and after 2 years of CO_2 injection. Line Source. Both figures are shown with the SAME SC

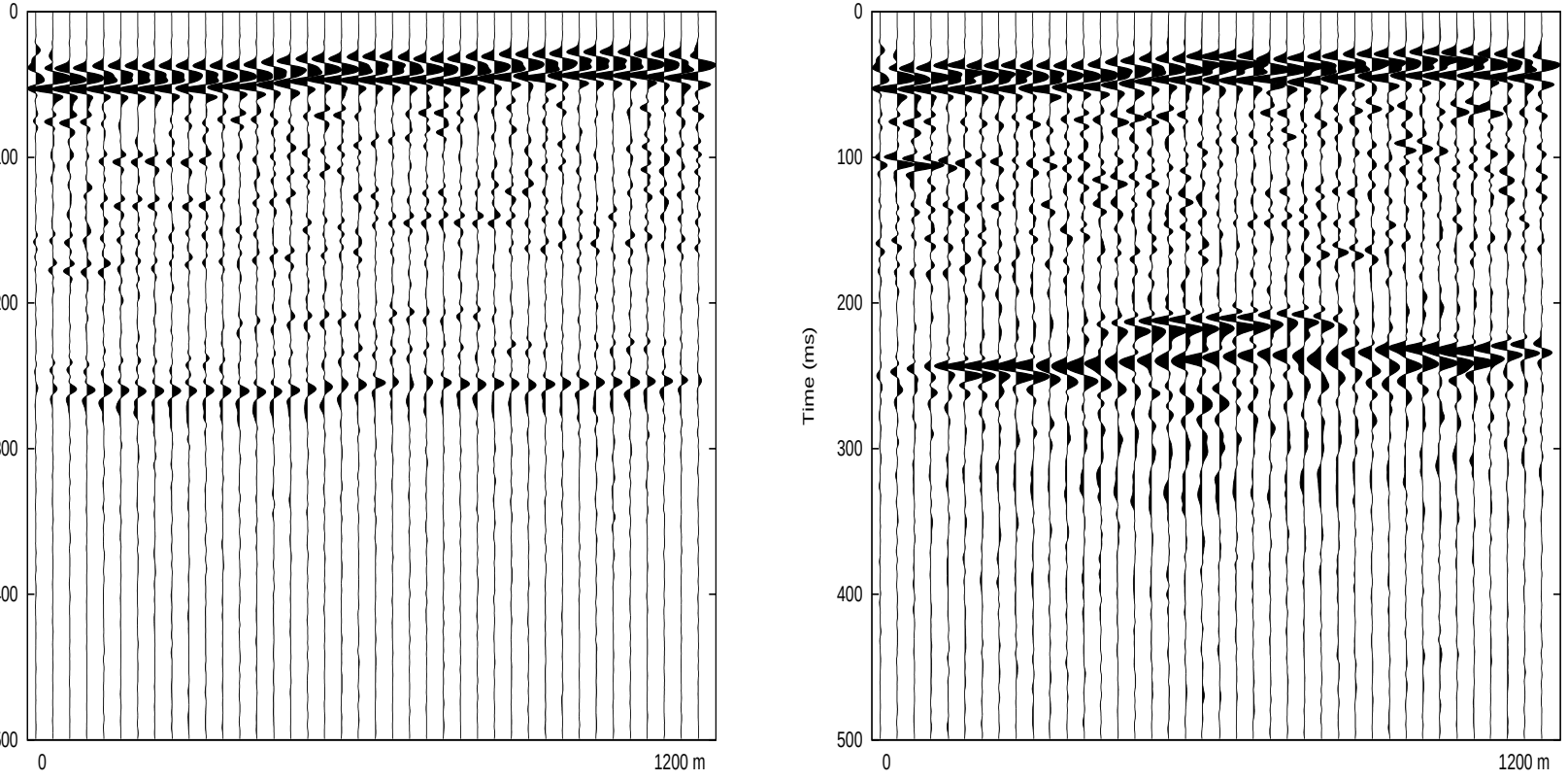

ces of the z-component of the particle velocity before (left) and after 2 years (right) CO_2 injection. The two

ivals seen on the left Figure come from the base and top of the Utsira. The strong later arrivals seen on the

ht Figure are due to P-waves reflected at CO_2 accumulations and the base of the Utsira.

histories before and after 2 and 6 years of CO_2 injection. Line Source

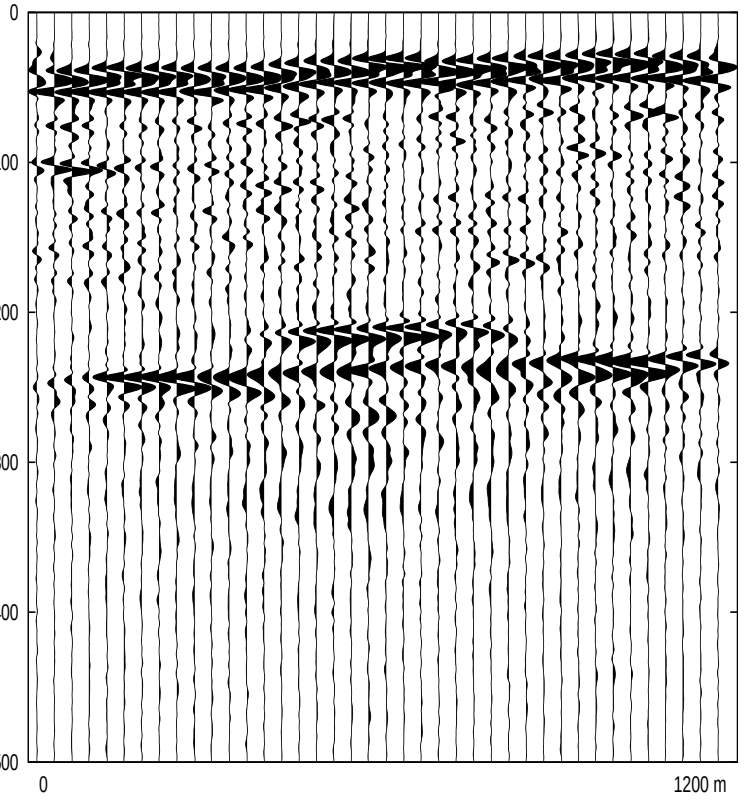

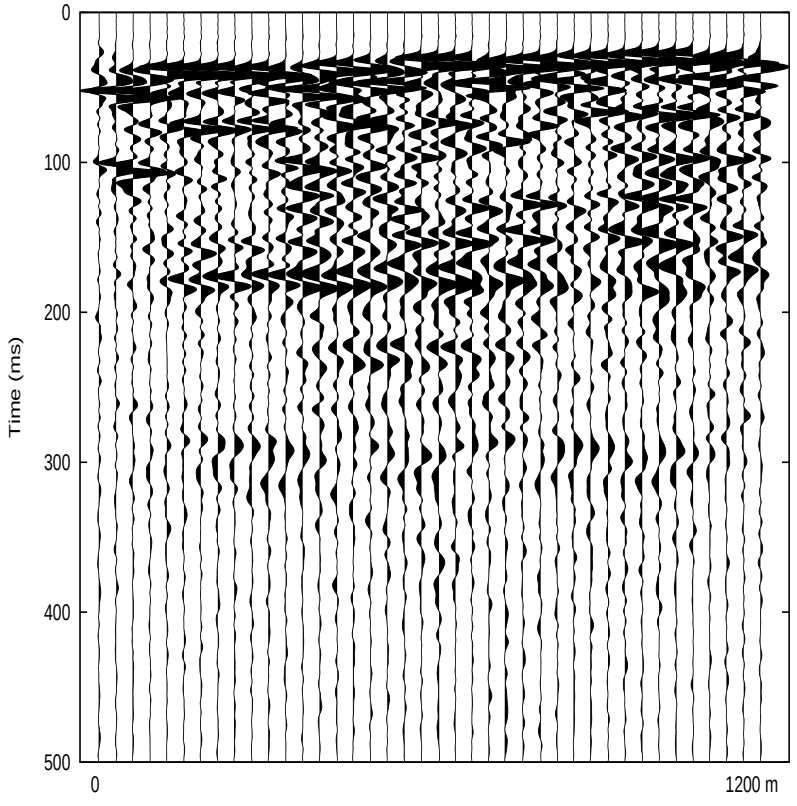

ces of the z-component of the particle velocity after 2 years (left) and 6 years (right) of CO_2 injection. The

lier arrivals on the right Figure are due to waves reflected at the CO_2 accumulations below the shalow

dstone layers.

ONCLUSIONS

- The numerical examples show the effectiveness of combining multiphasic flow simulators in porous media with seismic monitoring to map the spatio-temporal distribution of CO_2 after injection.
- The wave propagation model includes attenuation and dispersion effects due to mesoscopic scale heterogeneities using White's theory.
- This methodology constitutes a valuable tool to monitor the migration and dispersal of the CO_2 plume and to analyze storage integrity, providing early warning should any leakage occurs.

NOWLEDGEMENTS

his work was partially funded by CONICET, Universidad de
uenos Aires, Universidad Nacional de La Plata and the
uropean Union under project CO2 ReMoVe.

HANKS FOR YOUR ATTENTION !!!!!!